

Epi-direction detected multimodal imaging of an unstained mouse retina with a Yb-fiber laser

Gabrielle A. Murashova,¹ Christopher A. Mancuso,¹ Sanae Sakami,² Krzysztof Palczewski,² Grazyna Palczewska,³ and Marcos Dantus¹

¹Department of Chemistry, Michigan State University, East Lansing, MI, 48824, USA

²Department of Pharmacology, Case Western Reserve University, Cleveland OH 44106, USA

³ Department of Medical Devices, Polgenix Inc., Cleveland, OH 44106, USA

ABSTRACT

In this work, we present all epi-direction detected images of an unstained mouse retina using multiphoton microscopy with a sub-50 fs Yb-fiber laser centered at 1.07 μm . This wavelength is particularly interesting as the fundamental wavelength is transparent to the anterior segment of the eye and the higher harmonics are above DNA-damaging UV wavelengths. We present a characterization of the multimodal signals emitted from the different retinal layers, as well as from the choroid and the sclera. By characterizing native multiphoton signals from the retina, we move closer to having Yb-fiber considered for *in vivo* diagnosis of retinal disease through multiphoton microscopy as well as for corrective therapies.

Keywords: Retina; Second Harmonic Generation; JenLab Young Investigator Award; Ultrafast lasers; Multimodal; Biomedical imaging; Yb-fiber Laser.

1. INTRODUCTION

Multiphoton microscopy is an established technique that provides high-contrast imaging of unstained biomedical tissue samples.¹⁻⁶ Contrast arises from the fact that a tightly focused laser beam from ultrafast pulsed laser (< 1 ps) can generate signals through a number of nonlinear optical processes such as two-photon excited fluorescence (2PEF), three-photon excited fluorescence (3PEF), second harmonic generation (SHG), and third harmonic generation (THG). In the retina, the presence of 1.07 μm stimulated 2PEF can be attributed to visual pigments like rhodopsin present in photoreceptors outer segments and visual cycle byproducts like lipofuscin and A2E (the seventh product of the visual cycle).^{7,8} 3PEF emission is attributed to flavin adenine dinucleotide (FAD), and other endogenous fluorophores found in all living cells.^{7,9-12} In addition to endogenous fluorophores, harmonophores that lack an inversion center, such as the fibrous protein collagen, cause significant SHG emission.^{3,4}

In this Article, we present all epi-direction detected images of the retinal layers using an Yb-fiber laser with measured pulse durations below 50 fs. Shorter pulses lessen thermal damage while increasing multiphoton signals.¹³ By measuring the spectral components of the emitted light, we build a comprehensive picture of the emission of nonlinear signals driven by a Yb-fiber laser. Fiber lasers require no water-cooling, are less sensitive to air currents or changes in temperature, and their applications to three-photon processes are above the DNA damaging UV regime. While Ti: sapphire lasers have been used for multiphoton microscopy of the retina,¹⁴ their third-harmonic is centered at 266 nm, which matches the absorption maximum of DNA. By establishing the native multiphoton signals that arise from wild type *ex vivo* retinas, *in vivo* and clinical use for the diagnosis and treatment of retinal diseases, such as age-related macular degeneration (AMD) can be established.¹⁵

2. MATERIALS AND METHODS

The light source for our multiphoton microscope is an Yb-fiber laser oscillator (1.07 μm , 42 MHz).¹⁶ The custom cavity design of our laser allows for the production of pulses with a full-width at half-maximum pulse duration of 42 fs. For imaging we used a 40x water immersion objective with a working distance of 0.5 mm (Zeiss LD-C APOCHROMAT 1.1 NA, Jena, Germany) to focus the beam on the retina to a spot size of 0.5 μm , allowing for the generation of peak intensities high enough to induce multiphoton processes with less than 9 mW of average power, minimizing the effects of photobleaching and thermal damage. When using a photomultiplier (data not shown), multiphoton imaging with 3.2 mW of average power was sufficient. Laser scanning was done with galvanometer mirrors without blanking. The peak intensity was maximized through the use of a pulse-shaper (MIIPS HD, Biophotonic Solutions Inc., East Lansing,

Michigan) which accounted for the dispersion along the beam path.^{17,18} Photon detection was done in the epi-direction. To obtain images as well as the wavelength data of the collected photon signals we used a time-correlated single photon counting (SPC-830 TCSPC, Becker-Hickl, GmbH) detector, equipped with 16-PMTs. The wavelength range collected was from 485 nm to 685 nm.

We imaged a 5 μm -thick transverse slice of mouse retina mounted with optimal cutting temperature media on a microscope slide with a No. 1.5 cover glass using a Nikon TE2000 inverted microscope (Fig. 1). The retina was mounted such that the retinal layers were in a plane perpendicular to the laser propagation axis. Retinal sections were prepared at Case Western Reserve University (CWRU) and all animal procedures were approved by the CWRU Animal Care and Use Committee and complied with the American Veterinary Medical Association Guidelines on Euthanasia. Due to the fact that THG is emitted primarily in the forward direction, we were not able to detect THG signals from 5 μm -thick retina sections in the epi direction.¹⁹

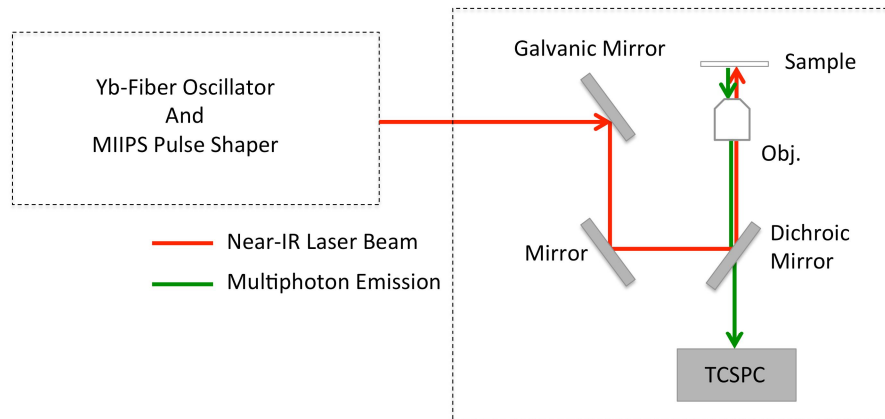


Fig.1. The experimental apparatus consists of an ultrafast fiber laser operating at 1.07 μm , a MIIPS pulse shaper, laser scanning microscope, and a time-correlated single photon counting (TCSPC) detector.

3. RESULTS AND DISCUSSION

Multiphoton imaging of the retinal layers, including the nerve fiber layer (NFL), ganglion cell layer (GCL), inner plexiform layer (IPL), inner nuclear layer (INP), outer plexiform layer (OPL), outer nuclear layer (ONL), receptor layer (RL; comprised of the inner and outer segment layers), and retinal pigmented epithelium (RPE) is shown in Fig. 2. In addition to the retina layers we imaged both the choroid and the sclera. The emitted signals were grouped into two wavelength ranges; the red and green, which correspond to wavelengths 565 nm to 685 nm, and 500 nm to 565 nm, respectively (Fig. 2 and Fig. 3a).

The emitted signals across most of the retinal layers (RL to NFL) are fairly uniform, showing an equal contribution from signals emitted at 500-560 nm and 590-685 nm (yellow colored region in Fig. 2 and Fig. 3a). In these regions we attribute the emission at 500-565 nm to 2PEF of rhodopsin and 3PEF of all-*trans*-retinol (both present in photoreceptors' outer segments), as well as 3PEF of FAD.⁸ The emission at 565-685 nm is attributed to hemoglobin, as well as yet to be identified fluorophores.^{12,20-24} In comparison, the remaining layers demonstrate more complexity to their multiphoton emission.

In the RPE there is a 2PEF emission in the range of 565-685 nm, which is due to a large source of lipofuscin ($\lambda_{\text{em}}=585\text{-}610\text{ nm}$) and its components like A2E ($\lambda_{\text{em}}=620\text{-}630\text{ nm}$).^{12,20,22-24} Lipofuscin is a lysosomal fluorophore that accumulates in the RPE as a result of phagocytosis of the disk membranes that make up the outer segments of photoreceptor cells.⁸ These lysosomal fluorophores include vitamin A and downstream degradation products such as A2E.^{7,22,25-27}

In addition to the RPE, the choroid also emits signals that are within the 565-685 nm range. The choroid makes up the vascular system of the outer retina, where nutrients, oxygen, and waste are transported to and from the retinal layers.²¹ Hemoglobin, which is present in the choroid, fluoresces at wavelengths ($\lambda_{\text{exc}}=535\text{ nm}$, $\lambda_{\text{em}}=605\text{-}615\text{ nm}$) that contribute to the 2PEF red channel signal, along with A2E detected in the choroid.^{6,21} Because the sclera is the fibrous protective layer of the eye, the strong emission in the range of 500-565 nm is attributed to second harmonic signal generated *via* interaction with collagen.^{3,4}

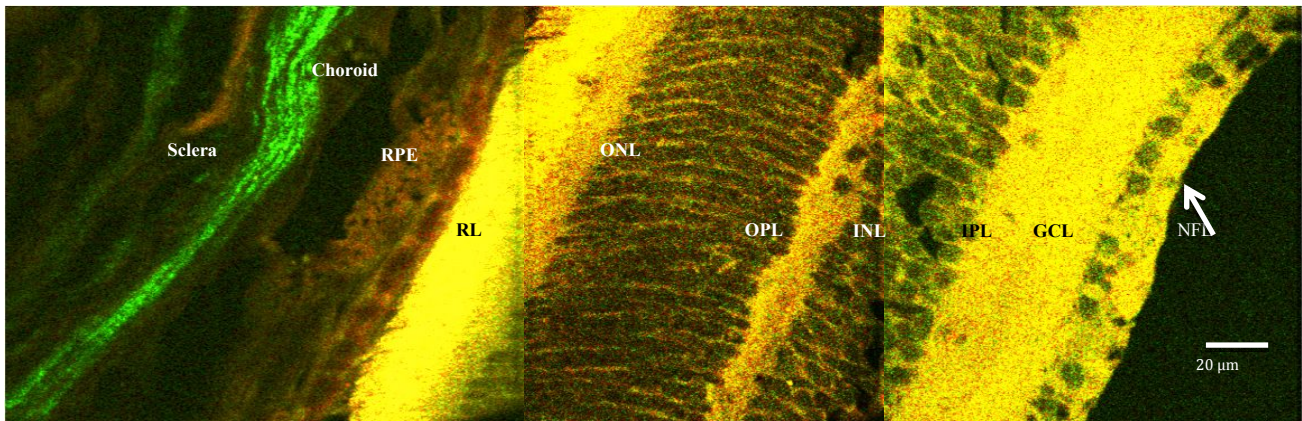


Fig. 2. Two color (red and green) false color image of the retinal layers taken with the TCSPC at 8.4 mW of laser power. The red channel contains emission from wavelengths 565 nm to 685 nm (lipofuscin, A2E, rhodopsin, vitamin A, and hemoglobin) and the green channel contains emission from 500 nm to 565 nm (FAD and collagen). The yellow regions correspond to equal signal strengths of the two channels.

To highlight the difference in the emitted multiphoton signals in a few different layers, we plot the full wavelength spectra for the sclera, RPE, and RL (Fig. 3b). The wavelength spectrum for the sclera shows that the majority of the signal in this region is centered around 535 nm, which agrees with the previously known collagen content of the sclera.^{3,4} The spectrum for the RPE is dominated by emission in the 565 to 685 nm range due to the large concentration of lipofuscin and A2E.^{12,20,22-24} The spectrum for the RL is a fairly equal mixture of emission from 500-565 nm and 565 to 685 nm. The RL membranes are densely packed with rhodopsin.⁸ Other fluorophores required for protection and function of the photoreceptors (rods and cones) such as all-*trans* retinol, NADPH, and FAD are also present within this layer.^{8,12,20-24}

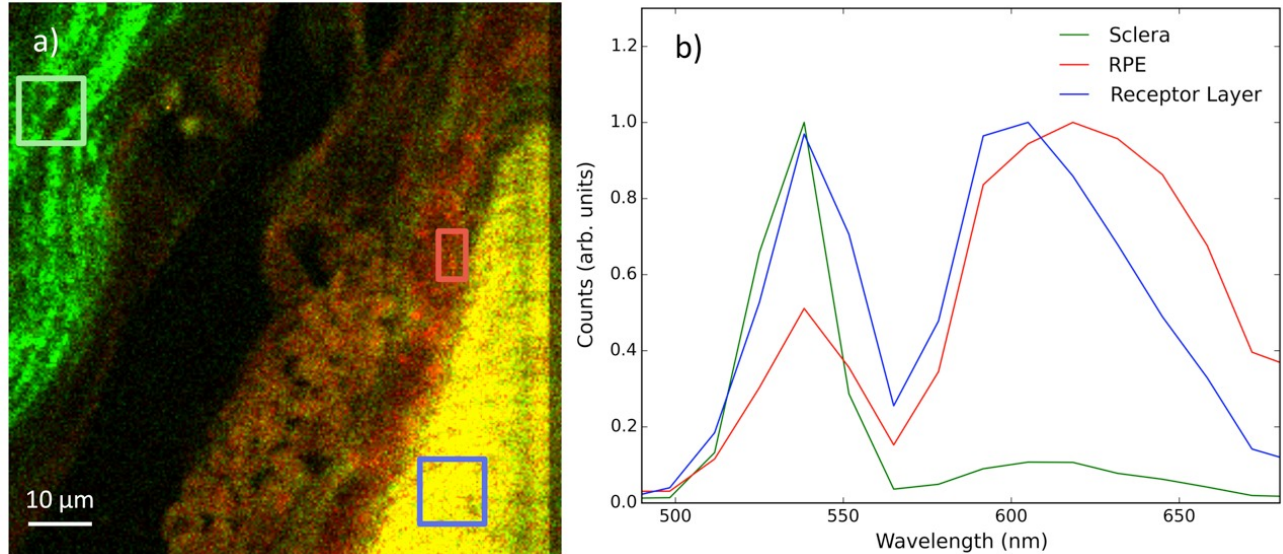


Fig. 3. (a) False-colored image of the sclera, choroid, RPE, and RL from an isolated mouse retina taken at 8.4 mW of power. The image is divided into two wavelength groups; green corresponds to wavelengths 500-565 nm, and red corresponding to wavelengths 565-685 nm. The yellow signal is due to equal amounts of emission from the two channels. (b) The wavelength distribution for each of the three, color-coded boxed areas in (a); green for the sclera, red for the RPE, and blue for the RL.

4. CONCLUSIONS

In summary, we present results of all epi-direction multiphoton imaging of an unstained isolated mouse retina with a sub-50 fs ultrafast Yb-fiber laser centered at 1.07 μm . The multimodal signals were identified through spectroscopic

photon analysis. These results present an in-depth characterization of endogenous nonlinear signals generated in the retina using an Yb-fiber laser. These results show one can acquire high-resolution and spectrally differentiated images of unstained retina with low exposure times. Epi-direction detection of multiphoton signals in unstained retina using an Yb-fiber laser suggests a viable transition of these lasers into a clinical setting.

ACKNOWLEDGEMENTS

Partial funding of this work comes from the National Science Foundation under grant CHE-1464807 for the development of novel spectroscopic methods and from National Institutes of Health grant U01 EY025451. CAM is thankful for his support from Michigan State University. Additionally, GAM is thankful for the opportunity to compete for the JenLab Young Investigator Award.

REFERENCES AND LINKS

- [1] Denk, W., Strickler, J. H., Webb, W. W., "Two-photon laser scanning fluorescence microscopy.," *Science* **248**(4951), 73–76 (1990).
- [2] Müller, M., Squier, J., Wilson, K. R., Brakenhoff, G. J., "3D microscopy of transparent objects using third-harmonic generation," *J. Microsc.* **191**(3), 266–274 (1998).
- [3] Williams, R. M., Zipfel, W. R., Webb, W. W., "Interpreting second-harmonic generation images of collagen I fibrils.," *Biophys. J.* **88**(2), 1377–1386, The Biophysical Society (2005).
- [4] Rocha-Mendoza, I., Yankelevich, D. R., Wang, M., Reiser, K. M., Frank, C. W., Knoesen, A., "Sum Frequency Vibrational Spectroscopy: The Molecular Origins of the Optical Second-Order Nonlinearity of Collagen," *Biophys. J.* **93**(12), 4433–4444 (2007).
- [5] Gibson, E. A., Masihzadeh, O., Lei, T. C., Ammar, D. A., Kahook, M. Y., "Multiphoton microscopy for ophthalmic imaging.," *J. Ophthalmol.* **2011**, 870879, Hindawi Publishing Corporation (2011).
- [6] Saytashev, I., Glenn, R., Murashova, G. A., Osseiran, S., Spence, D., Evans, C. L., Dantus, M., "Multiphoton excited hemoglobin fluorescence and third harmonic generation for non-invasive microscopy of stored blood," *Biomed. Opt. Express* **7**(9), 3449, Optical Society of America (2016).
- [7] Katz, M. L., Gao, C.-L., Rice, L. M., "Formation of lipofuscin-like fluorophores by reaction of retinal with photoreceptor outer segments and liposomes," *Mech. Ageing Dev.* **92**(2), 159–174 (1996).
- [8] Palczewska, G., Vinberg, F., Stremplewski, P., Bircher, M. P., Salom, D., Komar, K., Zhang, J., Cascella, M., Wojtkowski, M., et al., "Human infrared vision is triggered by two-photon chromophore isomerization.," *Proc. Natl. Acad. Sci. U. S. A.* **111**(50), E5445-54, National Academy of Sciences (2014).
- [9] Boulton, M., Docchio, F., Dayhaw-Barker, P., Ramponi, R., Cubeddu, R., "Age-related changes in the morphology, absorption and fluorescence of melanosomes and lipofuscin granules of the retinal pigment epithelium," *Vision Res.* **30**(9), 1291–1303 (1990).
- [10] Lakowicz, J. R., *Principles of fluorescence spectroscopy*, Third, Princ. Fluoresc. Spectrosc., Third, Springer, Baltimore (2006).
- [11] Becker, W., *The bh TCSPC Handbook*, sixth, Berlin (2010).

- [12] Sparrow, J. R., Wu, Y., Nagasaki, T., Yoon, K. D., Yamamoto, K., Zhou, J., “Fundus autofluorescence and the bisretinoids of retina,” *Photochem. Photobiol. Sci.* **9**(11), 1480–1489 (2010).
- [13] Nie, B., Saytashev, I., Chong, A., Liu, H., Arkhipov, S. N., Wise, F. W., Dantus, M., “Multimodal microscopy with sub-30 fs Yb fiber laser oscillator,” *Nat. Biotechnol. J. Microsc* **248**(2002), 73–76 (1990).
- [14] He, S., Ye, C., Sun, Q., Leung, C. K. S., Qu, J. Y., “Label-free nonlinear optical imaging of mouse retina,” *Biomed. Opt. Express* **6**(3), 1055 (2015).
- [15] Masihzadeh, O., Ammar, D. A., Kahook, M. Y., “Coherence-Gated Sensorless Adaptive Optics Multiphoton Retinal Imaging Coherent Anti-Stokes Raman Scattering (CARS) Microscopy : A Novel Technique for Imaging the Retina,” *Invest. Ophthalmol. Vis. Sci.* **54**(5), 3094–3101 (2013).
- [16] Nie, B., Pestov, D., Wise, F. W., Dantus, M., “Generation of 42-fs and 10-nJ pulses from a fiber laser with self-similar evolution in the gain segment,” *Opt. Express* **19**(13), 12074–12080, Optical Society of America (2011).
- [17] Lozovoy, V. V., Pastirk, I., Dantus, M., “Multiphoton intrapulse interference. IV. Ultrashort laser pulse spectral phase characterization and compensation,” *Opt. Lett.* **29**(7), 775–777, Optical Society of America (2004).
- [18] Biophotonic Solutions., Pulse Compression for Ultrafast Nonlinear Microscopy, 1.2, Biophotonic Solutions Inc. (2015).
- [19] Boyd, R. W., *Nonlinear Optics*, Book, Academic Press, Rochester (2008).
- [20] Kennedy, C. J., Rakoczy, P. E., Constable, I. J., “Lipofuscin of the retinal pigment epithelium: a review.,” *Eye (Lond)*. **9**, 763–771 (1995).
- [21] Flower, R., Rudolph, A. S., “Effects of free and liposome-encapsulated hemoglobin on choroidal vascular plexus blood flow, using the rabbit eye as a model system.,” *Eur. J. Ophthalmol.* **9**(2), 103–114 (1999).
- [22] Lin, E. H. B., Von Korff, M., Peterson, D., Ludman, E. J., Ciechanowski, P., Katon, W., “Population targeting and durability of multimorbidity collaborative care management,” *Am. J. Manag. Care* **20**(11), 887–893 (2014).
- [23] Palczewska, G., Dong, Z., Golczak, M., Hunter, J. J., Williams, D. R., Alexander, N. S., Palczewski, K., “Noninvasive two-photon microscopy imaging of mouse retina and retinal pigment epithelium through the pupil of the eye,” *Nat. Med.* **20**(7), 785–789, Nature Research (2014).
- [24] Sparrow, J., Duncker, T., “Fundus Autofluorescence and RPE Lipofuscin in Age-Related Macular Degeneration,” *J. Clin. Med.* **3**(4), 1302–1321, Multidisciplinary Digital Publishing Institute (2014).
- [25] Robison, W. G., Katz, M. L., “Vitamin A and Lipofuscin,” Springer New York, 95–122 (1987).
- [26] Holz, F., Spaide, R., Bird, A. C., Smitz-Valckenberg, S., “Lipofuscin of the Retinal Pigment Epithelium,” [Atlas of Fundus Autofluorescence Imaging], Frank Holz, Richard Spaide, Alan C. Bird, and Steffen Smitz-Valckenberg, Eds., Springer Berlin Heidelberg, Berlin, Heidelberg, 3–16 (2007).
- [27] Boulton, M. E., “Studying melanin and lipofuscin in RPE cell culture models.,” *Exp. Eye Res.* **126**, 61–67, NIH Public Access (2014).